JACS
JOURNAL OF THE AMERICAN CHEMICAL SOCIETY
Article
pubs.acs.org/JACS

Fabrication of COF-MOF Composite Membranes and Their Highly Selective Separation of H_2/CO_2

Jingru Fu,[†] Saikat Das,[†] Guolong Xing,[†] Teng Ben,*[,†] Valentin Valtchev,[†,‡] and Shilun Qiu[†]

[†]Department of Chemistry, Jilin University, 130012 Changchun, China

[‡]Normandie Univ, ENSICAEN, UNICAEN, CNRS, Laboratoire Catalyse et Spectrochimie, 14000 Caen, France

Supporting Information

ABSTRACT: The search for new types of membrane materials has been of continuous interest in both academia and industry, given their importance in a plethora of applications, particularly for energy-efficient separation technology. In this contribution, we demonstrate for the first time that a metal−organic framework (MOF) can be grown on the covalent-organic framework (COF) membrane to fabricate COF-MOF composite membranes. The resultant COF-MOF composite membranes demonstrate higher separation selectivity of H_2/CO_2 gas mixtures than the individual COF and MOF membranes. A sound proof for the synergy between two porous materials is the fact that the COF-MOF composite membranes surpass the Robeson upper bound of polymer membranes for mixture separation of a H_2/CO_2 gas pair and are among the best gas separation MOF membranes reported thus far.

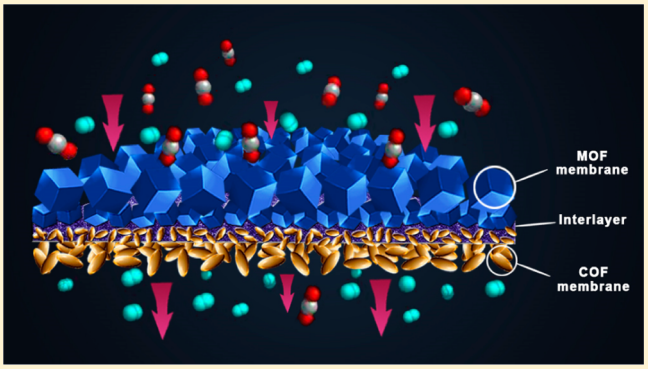

INTRODUCTION

Over the past two decades, there has been an upsurge in the development and use of membranes for research-oriented and industrial applications.[1−4] A membrane is a partition or wall that selectively controls the passage of different entities through it and is generally employed for the purpose of separation. The major advantage of membrane separation over other separation methods lies in energy/cost efficiency. Recently there has been an escalating interest in developing metal−organic frameworks (MOFs) as membranes due to their structural diversity, uniform pore sizes, functionalizable pore walls, and thus exceptional separation properties.[5] MOF membranes have been extensively explored for usage in gas,[6−13] liquid,[14] and ion[15] separations owing to their controllable pores and chemical selectivity.[5] Zeolitic imidazolate frameworks (ZIFs),[16] a subfamily of MOFs, have lately emerged as an important group of porous materials for the fabrication of membranes.[17−27] The high interest is exemplified by the preparation, among others, of ZIF-7,[17,18] ZIF-8,[19−21] ZIF-22,[22] ZIF-90,[23−25] ZIF-95,[26] and ZIF-100[27] membranes, which demonstrated high gas separation capabilities.

Covalent organic frameworks (COFs) represent a new type of porous materials comprising strong covalent bonds between light elements (C, B, N, O, Si, etc.).[28,29] Credited with outstanding structural flexibility, large surface area, tunable pore size, remarkably high thermal stability, and low density,[30] COFs in various forms, namely powders[31] and thin films,[31−34] have been widely investigated for applications in gas storage and separation,[35,36] catalysis,[37,38] and energy storage.[39]

Carbon dioxide is a greenhouse gas that in the long term could have devastating consequences on the environment. The capture of carbon dioxide is a straightforward solution to restrain its harmful effect on the environment.[40,41] The precombustion carbon capture involves the reaction of syngas[41] (comprising H_2 and CO) with steam, yielding H_2 and CO_2. The polymer membranes endowed with effective gas separation selectivity for CO_2 and H_2[41,42] can be employed for the capture of CO_2 while H_2 is subjected to combustion, indicating its applicability as a clean fuel.[40−42]

Albeit there has been considerable advancement in membrane-based gas separation using porous materials such as MOFs, COFs, etc., it remains a great challenge to fabricate membranes with both high selectivity and high permeability. In 1991, L. M. Robeson[43] identified an upper bound relationship (revisited in 2008[44]) to specify the limits of gas separation by polymer membranes, which goes as $P_i = k\alpha_{ij}^n$, where P_i represents the permeability of the more permeable gas, α_{ij} represents the separation factor P_i/P_j, k represents the front factor of the relationship, and n represents the slope of the log−log plot from the relationship. Similar to other limits in science, the upper bound relationship has been inspiring a lot of research with the aim to surpass it.

Herein we present the fabrication of the novel COF-MOF composite membranes, which not only demonstrate higher selectivity of H_2/CO_2 gas mixtures than the respective COF

Received: March 31, 2016
Published: May 26, 2016

DOI: 10.1021/jacs.6b03348
J. Am. Chem. Soc. 2016, 138, 7673−7680

and MOF membranes but also surpass the Robeson upper bound of polymer membranes for mixture separation of the H_2/CO_2 gas pair. This excellent performance is rationalized in terms of the chemical nature of the building components (support, COF, MOF) and their interactions at the interface between different layers.

EXPERIMENTAL SECTION

Fabrication of COF membrane. First, porous SiO_2 disks (25 mm diameter, 4 mm thickness) were polished with emery paper (mesh 500 followed by mesh 1200) until the diameter was 15 mm, the thickness was 2 mm, and the upper face of the disks was well polished. After this, three of these disks were immersed in distilled water (100 mL) followed by 3 rounds of ultrasonic washing, each round lasting 20 min. The disks were subsequently washed three times with anhydrous ethanol (50 mL), each time for 30 min, and then oven-dried at 70 °C overnight. Next the polyaniline (PANI) powder was dissolved in dimethylformamide (DMF) to obtain a supersaturated solution of PANI and the smooth face of the SiO_2 disks was coated with the resulting solution by dropper. The disks were then oven-dried at 70 °C. The coating step followed by oven-drying of the disks was repeated three times. The SiO_2 disks processed with PANI will be referred to as PANI-modified SiO_2 disks hereinafter.

Terephthalaldehyde (36.00 mg, 0.27 mmol) and tetra-(4-anilyl)-methane (60.00 mg, 0.16 mmol) were dissolved in anhydrous 1,4-dioxane (3.00 mL). 0.60 mL of a 3.00 M aqueous solution of acetic acid was added to the above mixture under vigorous stirring, and the resulting solution (COF-300 mother solution) was introduced in a Teflon-lined autoclave (25 mL). The PANI-modified porous SiO_2 disk was then placed horizontally face up in the autoclave and heated at 100 °C for 3 days. The resulting membrane was subsequently washed with anhydrous 1,4-dioxane and anhydrous tetrahydrofuran several times and dried in air at room temperature.

Fabrication of MOF membrane. The $Zn_2(bdc)_2(dabco)$ membrane was fabricated as follows: $Zn_2(bdc)_2(dabco)$ mother solution was prepared by mixing zinc nitrate hexahydrate (594.90 mg, 2.00 mmol), terephthalic acid (332.00 mg, 2.00 mmol), 1,4-diazabicyclo[2.2.2]octane (DABCO; 146.00 mg, 1.30 mmol), and DMF (47.60 mL) and introduced in the Teflon-lined autoclave (50 mL). After this, the PANI-modified SiO_2 disk was placed horizontally in the autoclave for growth at 120 °C for 2 days. The resulting membrane was subsequently washed with DMF, immersed in anhydrous methanol overnight, and finally dried in air at room temperature.

ZIF-8 mother solution was prepared by mixing zinc chloride (544.00 mg, 4.00 mmol), 2-methylimidazole (492.00 mg, 6.00 mmol), sodium formate (288.00 mg, 4.23 mmol), and methanol (41.00 mL) and introduced in the Teflon-lined autoclave (50 mL). Next the PANI-modified SiO_2 disk was placed horizontally in the autoclave for growth at 120 °C for 4 h. The resulting ZIF-8 membrane was washed with methanol and dried in air at room temperature.

Fabrication of COF-MOF composite membranes. To prepare the [COF-300]-[$Zn_2(bdc)_2(dabco)$] composite membrane, a PANI-modified porous SiO_2 disk with a COF-300 membrane grown on the surface was placed horizontally faced up in the Teflon-lined autoclave containing $Zn_2(bdc)_2(dabco)$ mother solution. The rest of the fabrication procedure is similar to the one used for the $Zn_2(bdc)_2(dabco)$ membrane. In pursuance of fabrication of a [COF-300]-[ZIF-8] composite membrane, a PANI-modified porous SiO_2 disk comprising a COF-300 membrane was placed horizontally face up in the Teflon-lined autoclave. The rest of the procedure follows the same approach used for the preparation of the ZIF-8 membrane.

The chemical reactions that take place during the fabrication of the COF-300 membrane, $Zn_2(bdc)_2(dabco)$ membrane, [COF-300]-[$Zn_2(bdc)_2(dabco)$] composite membrane, ZIF-8 membrane, and [COF-300]-[ZIF-8] composite membrane are shown in Schemes S1, S2, and S3 of the Supporting Information. The fabrication of COF-MOF composite membranes is illustrated schematically with a flow diagram (Figure 1).

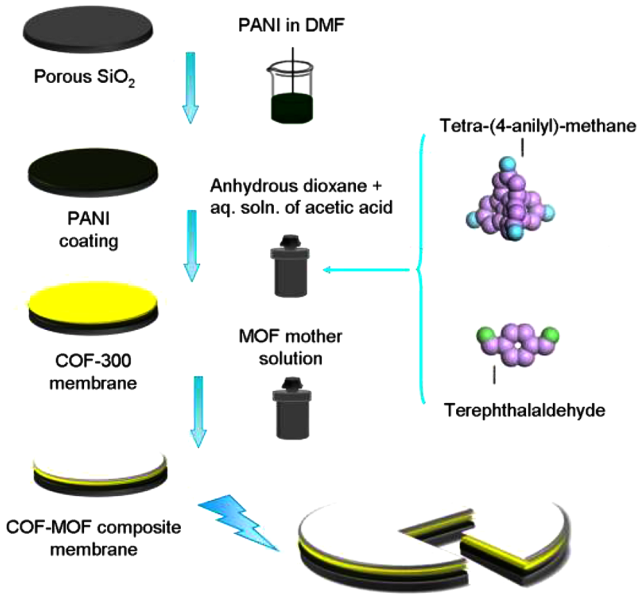

Figure 1. Schematic representation of the fabrication of COF-MOF composite membranes.

RESULTS AND DISCUSSION

The first stage of preparation of a composite membrane involves deposition of a layer of polyaniline on a SiO_2 disk. The second stage involves the condensation of polyaniline with terephthalaldehyde, eventuating in the development of an imine bond with the elimination of water. Then the free aldehyde groups react with tetra-(4-anilyl)-methane to yield a continuous and uniform layer of COF-300. The role of the polyaniline layer is to anchor the COF-300 crystals via the formation of imine groups (see Scheme S1 of the Supporting Information). The polyaniline coating is one of the key points of the preparation method because it not only adheres the porous SiO_2 tightly but also provides a functional surface full of dense amine groups. Such a dense amine layer further reacts with the aldehyde group to produce a defect-free continuous COF membrane with high selectivity.

In terms of the fabrication of the [COF-300]-[$Zn_2(bdc)_2(dabco)$] composite membrane, the terephthalic acid (one of the reagents used for the synthesis of $Zn_2(bdc)_2(dabco)$) forms a hydrogen bond[45,48] (Scheme S2 of the Supporting Information) with the amine group in COF-300, thereby facilitating the attachment of the top layer built of MOF crystals. Besides the hydrogen interactions, the sealing between the COF and MOF components of the membrane is promoted by the interaction of zinc cation with the amine group[20] (Scheme S2 of the Supporting Information). Similarly for the fabrication of the [COF-300]-[ZIF-8] composite membrane, the first step includes the reaction of zinc cation with an amine ($-NH_2$) group.[17,20,46] This statement is in agreement with the result of an FTIR study showing that the interaction between COF-300 powder and Zn results in the appearance of a Zn−N coordinate bond at 421 cm^{-1} (Figure S3). The Zn cations further react with the imidazole group in 2-methylimidazole to form a continuous and uniform layer of

DOI: 10.1021/jacs.6b03348
J. Am. Chem. Soc. 2016, 138, 7673−7680

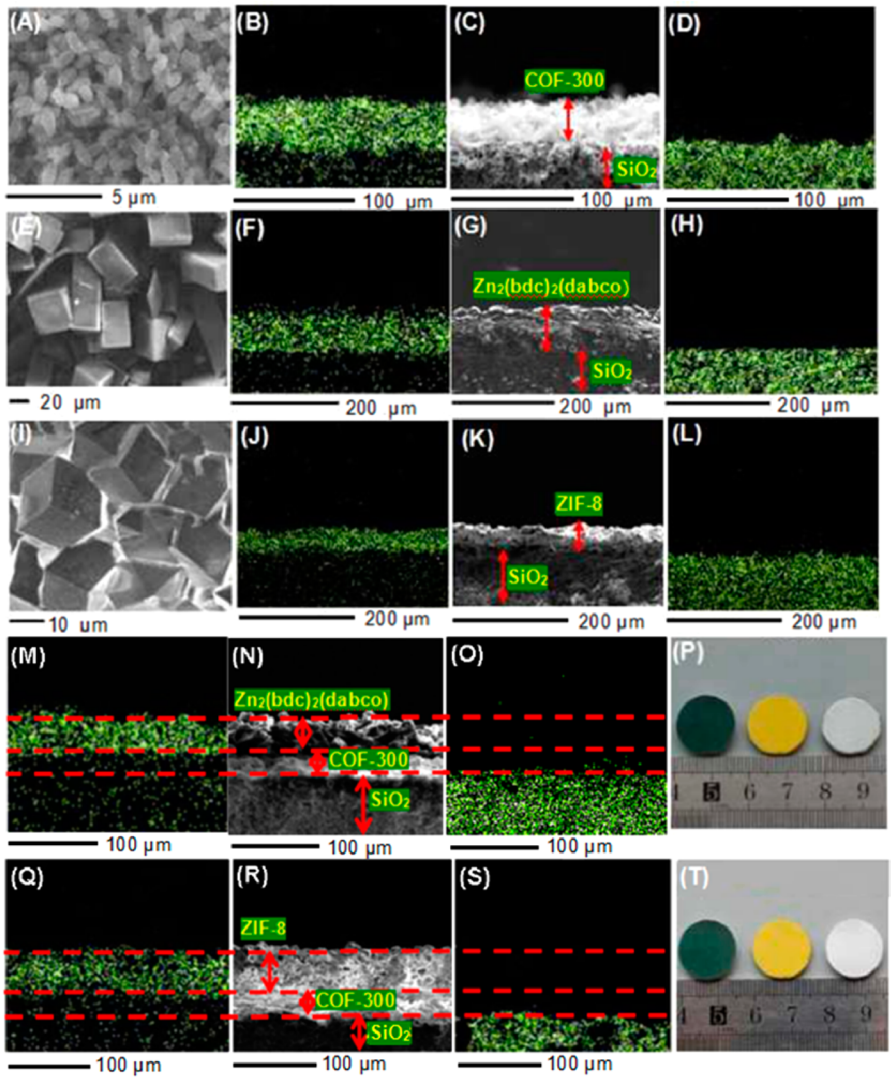

Figure 2. COF-300 membrane: (A) SEM top view, (B) elemental mapping image (carbon), (C) SEM cross-sectional view, and (D) elemental mapping image (silicon). $Zn_2(bdc)_2(dabco)$ membrane: (E) SEM top view, (F) elemental mapping image (zinc), (G) SEM cross-sectional view, and (H) elemental mapping image (silicon). ZIF-8 membrane: (I) SEM top view, (J) elemental mapping image (zinc), (K) SEM cross-sectional view, and (L) elemental mapping image (silicon). [COF-300]-[$Zn_2(bdc)_2(dabco)$] composite membrane: (M) elemental mapping image (zinc), (N) SEM cross-sectional view, (O) elemental mapping image (silicon), and (P) photo image. [COF-300]-[ZIF-8] composite membrane: (Q) elemental mapping image (zinc), (R) SEM cross-sectional view, (S) elemental mapping image (silicon), and (T) photo image.

ZIF-8 on the COF-300 layer (Scheme S3 of Supporting Information). In the present study, two types of MOFs have been grown on the COF-300 layer, highlighting the generality of the method. The two COF-MOF composite membranes exhibit similar characteristic features in spite of the differences in fabrication chemistry, which proves the versatility of this synthesis approach.

The successful fabrication of COF, MOF, and COF-MOF composite membranes has been confirmed by scanning electron microscopy (SEM) analysis, as illustrated in Figure 2. The uniformity and the thickness of different layers, e.g. MOF and COF, are evident from the cross-sectional SEM images of the composite membrane (Figure 2N, R). The thicknesses of the COF layer and the MOF layer corresponding to the [COF-300]-[$Zn_2(bdc)_2(dabco)$] composite membrane are about 42 and 55 μm, respectively. Similar thicknesses of these layers are observed in the case of the [COF-300]-[ZIF-8] composite membrane, where the COF and MOF layers are about 40 and 60 μm, respectively. The crystallinity of the COF-MOF composite membranes was studied by X-ray diffraction (XRD) analysis, which showed the expected diffraction peaks of MOF, COF-300, and SiO_2 materials (Figure S7). No other crystalline phase was detected. In the XRD patterns for the individual COF and MOF membranes, we observed solely the diffraction peaks for the COF layer and MOF layer, respectively. In the COF-MOF composite membrane, we obtained the diffraction peaks of the MOF material (Figure S7). This result indicates that the top of the composite membranes is built of pure MOF phase and the COF layer is covered completely by the MOF layer. N_2 sorption measurements were performed to evaluate the porosity of COF-300, $Zn_2(bdc)_2(dabco)$, and ZIF-8 powders obtained under conditions similar to those for the respective membrane fabrication (Figures S9, S10, and S11). All samples showed high porosity.

In regard to the gas permeance measurements, the stage cut, which is described by the ratio of permeate flow rate to feed flow rate, was maintained below 1% as a consequence of

DOI: 10.1021/jacs.6b03348
J. Am. Chem. Soc. 2016, 138, 7673−7680

emitting upstream of permeation cell via a soapfilm flowmeter.[47] Figure 3 shows the single gas permeabilities of

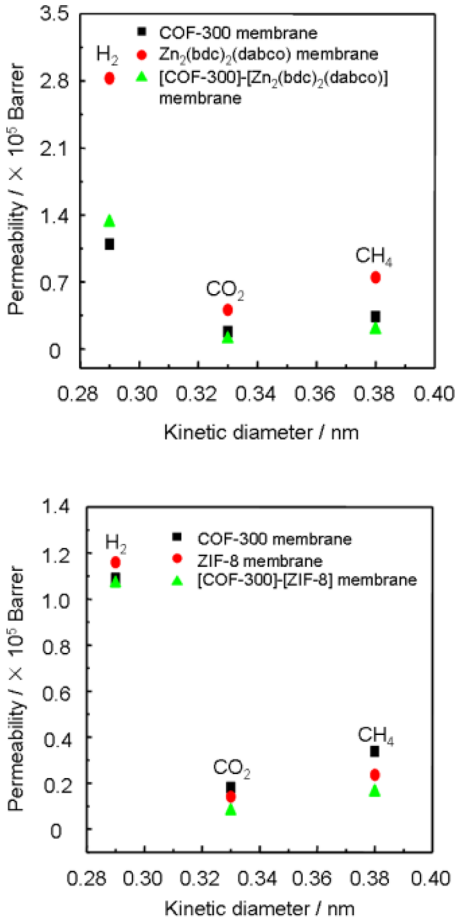

Figure 3. (top) Single gas permeability of various gases through the COF-300 membrane, $Zn_2(bdc)_2(dabco)$ membrane, and [COF-300]-[$Zn_2(bdc)_2(dabco)$] composite membrane at room temperature and 1 bar as a function of their kinetic diameters. (bottom) Single gas permeability of various gases through the COF-300 membrane, ZIF-8 membrane, and [COF-300]-[ZIF-8] composite membrane at room temperature and 1 bar as a function of their kinetic diameters.

H_2, CO_2, and CH_4 through the COF membrane, MOF membrane, and COF-MOF composite membranes as a function of the kinetic diameters of permeating gas molecules. We experimentally measured the single gas permeances through the COF, MOF, and COF-MOF composite membranes at room temperature and then determined the permeabilities of the corresponding membranes by multiplying the obtained value by the corresponding thicknesses of the membranes (see Equation S2 of the Supporting Information). The thicknesses of the selective layers corresponding to the COF-300 membrane, $Zn_2(bdc)_2(dabco)$ membrane, ZIF-8 membrane, [COF-300]-[$Zn_2(bdc)_2(dabco)$] composite membrane, and [COF-300]-[ZIF-8] composite membrane are about 45 μm, 120 μm, 60 μm, 97 μm, and 100 μm, respectively. The thicknesses of the composite membranes are evaluated by the sum of the thicknesses of the interlayer and the COF and MOF layers. The permeability of H_2 gas surpasses that of the other gases (CO_2 and CH_4), which is attributed to the smaller kinetic diameter of H_2. The gas separation capability of the COF-MOF composite membranes was evaluated by the separation of a 1:1 binary gas mixture of H_2/CO_2 at room temperature and 1 bar. As shown from Table 1, the mixture separation factor of H_2/CO_2 for the [COF-300]-[$Zn_2(bdc)_2(dabco)$] composite membrane is 12.6, which greatly surpasses those for the COF-300 membrane (6.0) and the $Zn_2(bdc)_2(dabco)$ membrane (7.0). The mixture separation factor of the H_2/CO_2 gas pair for the [COF-300]-[ZIF-8] composite membrane is 13.5, which markedly outperforms those for the COF-300 membrane (6.0) and the ZIF-8 membrane (9.1).

Several research groups have reported on the fabrication of MOF membranes using polymer-functionalized substrates. The major advantage of this approach is high compatibility between the polymer and MOF material. Thus, MOF membrane fabrication is facile and easy to scale up. Besides, the MOF membranes grown on polymer substrates show improved separation selectivity. In 2012, our group reported the fabrication of poly(methyl methacrylate)−poly(methacrylic acid) supported, free-standing HKUST-1 membranes.[11] Later we reported the fabrication of MOF thin films using polyaniline.[48] Caro and co-workers reported the fabrication of alumina-supported ZIF-7 membranes[17] involving dip-coating of the alumina discs with aqueous solution comprising ZIF-7 nanoseeds and polyethylenimine. The membrane exhibited H_2/CO_2 selectivity of 6.5 at 200 °C. Using a similar fabrication approach, the same group reported alumina-supported ZIF-7 membranes with H_2/CO_2 selectivity of 13.6 at 220 °C.[18] Banerjee et al.[49] fabricated a ZIF-8@polysulfonate membrane with a H_2/CO_2 selectivity of 3.8. Coronas et al.[50] lately reported the development of ZIF-8 and ZIF-93 membranes. This group used P84 (polyimide) hollow fibers, thereby yielding ZIF-8@P84 and ZIF-93@P84 hollow fiber membranes, followed by annealing of the membranes. The annealed membranes revealed augmented H_2/CH_4 selectivity. Nair et al.[51] fabricated ZIF-90/Torlon membranes exhibiting gas separation selectivity. Chung et al.[52] reported a 50/50 (w/w) ZIF-7/polybenzimidazole membrane with a H_2/CO_2 selectivity of 7.2 at 35 °C. In the present work, it is worth mentioning that the individual COF and MOF membranes (especially ZIF-8

Table 1. Comparison of the Gas Separation Capabilities of a H_2/CO_2 Binary Mixture (1:1) at Room Temperature and 1 bar by the COF-300 Membrane, $Zn_2(bdc)_2(dabco)$ Membrane, ZIF-8 Membrane, [COF-300]-[$Zn_2(bdc)_2(dabco)$] Composite Membrane, and [COF-300]-[ZIF-8] Composite Membrane

	COF-300 membrane		$Zn_2(bdc)_2(dabco)$ membrane		ZIF-8 membrane		[COF-300]-[$Zn_2(bdc)_2(dabco)$] membrane		[COF-300]-[ZIF-8] membrane	
Knudsen constant	P (H_2)[a]	SF (H_2/CO_2)	P (H_2)[a]	SF (H_2/CO_2)	P (H_2)[a]	SF (H_2/CO_2)	P (H_2)[a]	SF (H_2/CO_2)	P (H_2)[a]	SF (H_2/CO_2)
4.7	1.1	6.0	2.8	7.0	1.2	9.1	1.3	12.6	1.1	13.5

[a]H_2 permeability in Barrer (10^5 Barrer); SF stands for separation factor. Permeability is calculated as the membrane permeance multiplied by the membrane thickness. 1 Barrer = 3.347×10^{-16} mol·m^{-1}·s^{-1}·Pa^{-1}.

DOI: 10.1021/jacs.6b03348
J. Am. Chem. Soc. 2016, 138, 7673−7680

membrane) also show impressive gas separation selectivity along with the composite COF-MOF membranes. The impressive gas separation selectivity of the ZIF-8 membrane can be attributed to the intermediate layer of polyaniline. Polyaniline has good film-forming property, and it is feasible to attain a thin and uniform ZIF-8 film on the surface of SiO_2 upon usage of polyaniline. Polyaniline is amphiphilic, whereas SiO_2 is hydrophilic in nature. Thus, the functionalization of SiO_2 with polyaniline allows the growth of a tight ZIF-8 layer on the support. This is related with the high concentration of amine groups in the skeleton of the polyaniline. Consequently, the Zn can react with the amine group effectively (Figures S4, S5), which is manifested by the shift of the N−H stretching vibration by about 20 cm^{-1} from high wavenumber to low wavenumber. After implementing the Zn cations in the polyaniline, the ZIF-8 layer can be effectively grown.

It has to be underlined that the COF-MOF composite membranes surpass the Robeson upper bound of polymer membranes for mixture separation of the H_2/CO_2 gas pair.[43,44] Figure 4 illustrates the H_2/CO_2 selectivity as a function of H_2

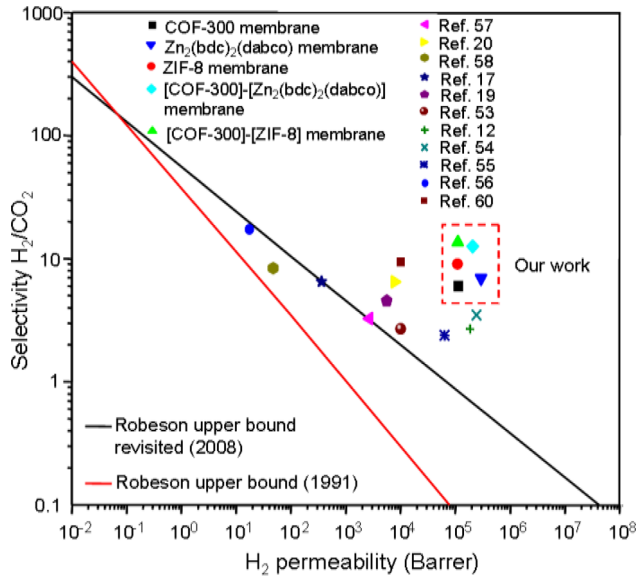

Figure 4. H_2/CO_2 selectivity as a function of H_2 permeability for our COF membrane, MOF membrane, and COF-MOF composite membranes compared with the membranes reported in the literature. The upper bound lines for polymer membranes are drawn according to refs 43 and 44. Permeability is calculated as the membrane permeance multiplied by the membrane thickness. One Barrer = 3.347×10^{-16} $mol \cdot m^{-1} \cdot s^{-1} \cdot Pa^{-1}$.

permeability for the COF-300 membrane, $Zn_2(bdc)_2(dabco)$ membrane, ZIF-8 membrane, [COF-300]-[$Zn_2(bdc)_2(dabco)$] composite membrane, and [COF-300]-[ZIF-8] composite membrane as well as the performance of other membranes reported in the literature.[12,17,19,20,53−58] COF-MOF composite membranes show high values in both permeability and selectivity in comparison with other membranes, thereby highlighting their potential for gas separation (Figure 4). It is worth mentioning that the COF-MOF composite membranes also show excellent selectivity in one single feeding of a gas mixture through the membranes as compared to some commercial membranes which need repeated stages of feeding of the gas mixture to achieve the desired selectivity. Some polymer membranes, such as the polyimide membranes reported by Shao et al.,[56] are facile to prepare, since they use ethylenediamine vapor to modify the membranes. The fabrication approach followed in the present study is also very convenient for fabrication; in addition, it is cost-efficient owing to the inexpensive chemicals used, and thereby, it is easy to scale up. The simple and rapid preparation of COF-MOF composite membranes represents another advantage over the conventional mixed matrix membranes (MMMs), whose fabrication usually takes several days.

MOF is prodigiously adopted to fabricate mixed matrix membranes for gas separation applications, owing to structural diversity and controllable pores, along with other advantages.[5] Huang et al.[59] reported the fabrication of a ZIF-8@graphene oxide membrane over a polydopamine-modified alumina support with a H_2/CO_2 selectivity of 14.9 at 250 °C. An alumina-supported ZIF-90 membrane synthesized comprising an intermediate layer of 3-aminopropyltriethoxysilane showed a H_2/CO_2 selectivity of 7.3 at 200 °C.[23] Knebel et al.[60] reported the fabrication of MIL-96(Al)@Matrimid MMMs with a H_2/CO_2 selectivity of about 6. In the present work, the individual COF and MOF membranes as well as the COF-MOF composite membranes fabricated on the surface of a polyaniline substrate show high selectivity combined with high permeability. This could be rationalized by a suitable binding energy between the porous framework and gas molecules, high porosity of COF and MOF, and fabrication of continuous membranes containing a few defects. The intent in the fabrication of COF-MOF composite membranes in the present study is to find synergy between different porous materials and thus higher gas separation selectivity than those of the individual, in the present case COF and MOF, membranes.

A pertinent question that arises at this point is why the composite membranes exhibit superior gas separation performance, as compared to those of individual single phase (COF or MOF) membranes. To gain a deeper understanding, the composite membranes were characterized by transmission electron microscopy (TEM) and *in situ* energy-dispersive X-ray spectroscopy (EDS). Figure 5(A) shows the TEM image along with fast Fourier transform (FFT) analysis (shown in insets) of the [COF-300]-[$Zn_2(bdc)_2(dabco)$] composite membrane. The inset (a) of Figure 5 illustrates the FFT of the white marked area. The FFT analysis reveals electron diffraction, giving the scalar value of the basis vector $\boldsymbol{a}^*$ of reciprocal space as 0.49. This value is analogous to the corresponding value of 0.5 (a = 20 Å for the COF-300 crystal[28]), which substantiates the fact that the white marked area is COF-300. As revealed by FFT, the interplanar spacing in the white marked area is 2.04 nm, which coincides with the N_2 adsorption result (2.00 nm, Figure S9). The inset (b) of Figure 5 illustrates the FFT of the red marked area. The FFT reveals no electron reflection, which confirms that the red marked area is amorphous. This result unambigously shows that there are two parts, a crystalline and an amorphous, in the composite layer. The crystalline part can be recognized by the lattice fringes and roundish morphology of COF-300 nanocrystalites, while the amorphous part is filling the space between shaped crystalline particles. The EDS spectrum of the amorphous part (see Figure S20 in the Supporting Information) reveals the presence of zinc, which points out the amorphous phase that fills up the gaps between COF crystals is MOF-type. The COF nanocrystalites are integrated in the amorphous matrix, and no interface between the two phases can be observed. The interlayer is schematically illustrated in Figure 5B. The set of

DOI: 10.1021/jacs.6b03348
J. Am. Chem. Soc. 2016, 138, 7673−7680

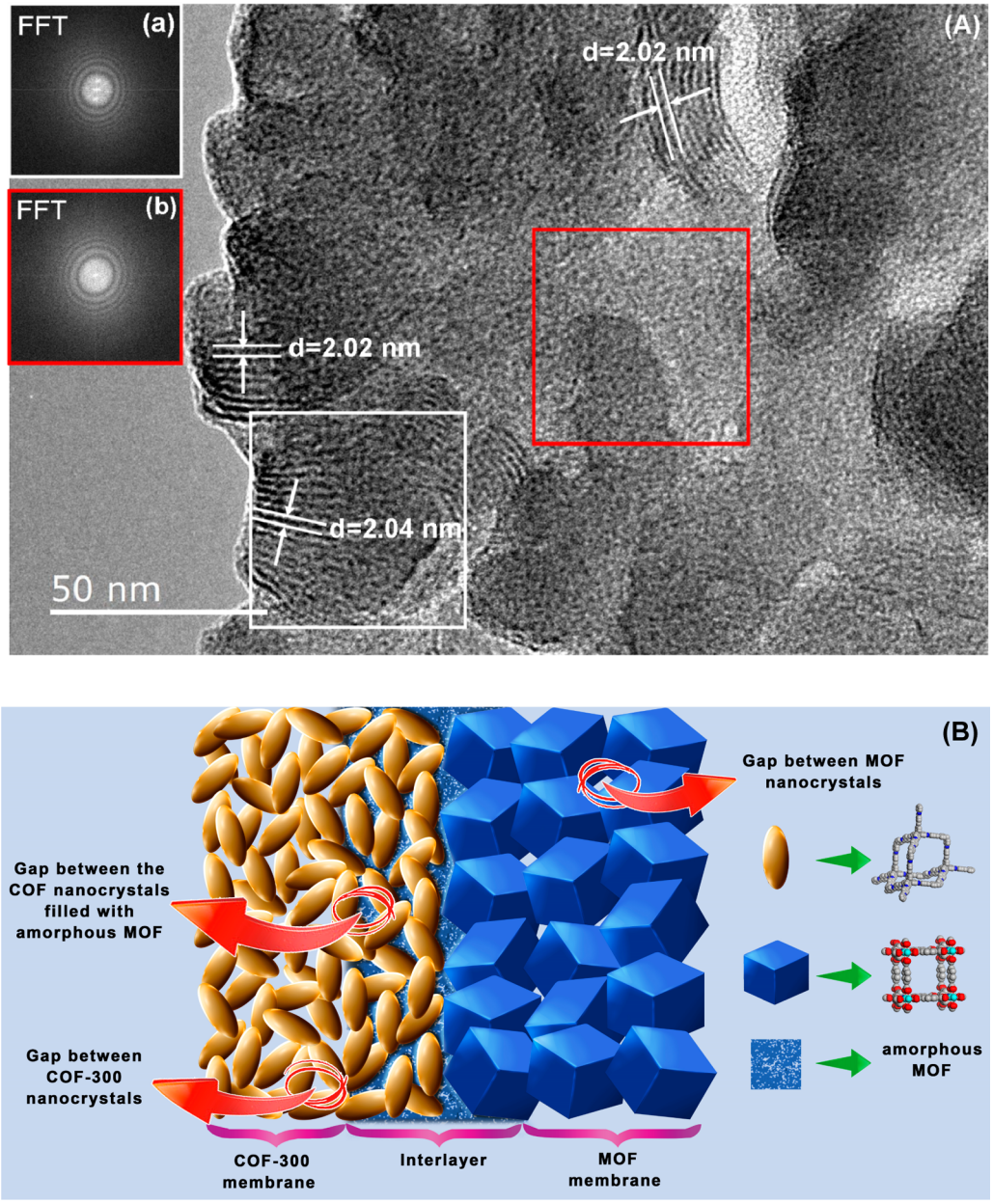

Figure 5. (A) TEM image and FFT analysis (shown in insets a,b) of the [COF-300]-[Zn_2(bdc)$_2$(dabco)] composite membrane. Inset (a) is the FFT of the white marked area, and inset (b) is the FFT of the red marked area. (B) Schematic illustration of the interlayer formed by amorphous MOF, which has similar pore size as a crystalline MOF, occupying the gaps between the COF nanocrystals and the interface between COF and MOF crystalline layers.

experimental data shows that the interlayer in the composite membrane is built up of COF-300 nanocrystalites and amorphous MOF material filling up the space between the nanocrystallites. The thicknesses of the COF layer, interlayer, and MOF layer corresponding to the [COF-300]-[Zn_2(bdc)$_2$(dabco)] composite membrane are about 42 μm, 200 nm, and 55 μm, respectively. Amorphous MOF[61,62] possesses similar pore size as that of crystalline MOF but lacks the long-range order. A possible reason for the formation of amorphous MOF is the mismatch of crystal parameters between COF and MOF, which leads to the disorder at the beginning of MOF nucleation. However, this amorphous MOF layer in the COF-MOF composite membranes is beneficial for membrane selectivity, since it seals the space between COF crystals, something that is difficult to be achieved if the MOF material was crystalline. Another important role of this layer is to maintain similar permeance (owing to similar pore size) to that of the individual COF and MOF layers.

■ CONCLUSION

This work is the first report on the fabrication of a COF membrane and a COF-MOF composite membrane. The COF-MOF composite membranes give higher selectivity of the H_2/CO_2 gas mixture than the individual COF and MOF counterparts. The mixture separation factors of a H_2/CO_2 (1:1) binary mixture through the [COF-300]-[Zn_2(bdc)$_2$(dabco)] and [COF-300]-[ZIF-8] composite membranes are 12.6 and 13.5, respectively, much higher than the separation factor values of 6.0, 7.0, and 9.1 for the respective COF-300, Zn_2(bdc)$_2$(dabco), and ZIF-8 membranes. The

DOI: 10.1021/jacs.6b03348
J. Am. Chem. Soc. 2016, 138, 7673−7680

separation factors are higher than that postulated by the Robeson upper bound limit of gas separation by polymer membranes. This remarkable performance is due to the method of fabrication, which involves the formation of chemical bonds between different components (support, COF, MOF) of the membrane. Namely, the COF crystals interact with polyaniline layer via imine groups, while HN-Zn-imidazole bonds seal the interface between COF and ZIF materials. In conclusion, the results of the present study show that a synergy between different molecular sieves materials can be found and thus much better performing membranes obtained. This approach can also certainly be extended to other couples of molecular sieves materials.

■ ASSOCIATED CONTENT

Supporting Information

The Supporting Information is available free of charge on the ACS Publications website at DOI: 10.1021/jacs.6b03348.

Chemical reactions during fabrication of membranes, Figures S2−S5 (FTIR measurements), Figures S6−S7 (XRD measurements), Figures S8 (TGA), Figures S9−S11 (N_2 sorption measurements), Figures S12−S14 (H_2, CO_2, and CH_4 sorption measurements), gas separation measurements, and Figure S20 (EDS spectrum) (PDF)

■ AUTHOR INFORMATION

Corresponding Author

*tben@jlu.edu.cn

Notes

The authors declare no competing financial interest.

■ ACKNOWLEDGMENTS

Financial support from the National Natural Science Foundation of China (Grant no. 21390394, 21261130584, 21471065), the National Basic Research Program of China (2012CB821700), and the "111" project (B07016) is gratefully acknowledged. V.V. acknowledges the financial support of the Micro-Green project (ANR-12-IS08-0001-01). The authors thank Dr. Liangkui Zhu for the discussion on FFT analysis.

■ REFERENCES

(1) Kölsch, P.; Venzke, D.; Noack, M.; Toussaint, P.; Caro, J. *J. Chem. Soc., Chem. Commun.* **1994**, 2491−2492.
(2) Huang, A. S.; Liu, Q.; Wang, N.; Caro, J. *J. Mater. Chem. A* **2014**, *2*, 8246−8251.
(3) Liu, Y.; Wang, N.; Diestel, L.; Steinbach, F.; Caro, J. *Chem. Commun.* **2014**, *50*, 4225−4227.
(4) Liu, Y.; Wang, N.; Caro, J. *J. Mater. Chem. A* **2014**, *2*, 5716−5723.
(5) Qiu, S.; Xue, M.; Zhu, G. *Chem. Soc. Rev.* **2014**, *43*, 6116−6140.
(6) Huang, A. S.; Chen, Y.; Liu, Q.; Wang, N.; Jiang, J.; Caro, J. *J. Membr. Sci.* **2014**, *454*, 126−132.
(7) Ranjan, R.; Tsapatsis, M. *Chem. Mater.* **2009**, *21*, 4920−4924.
(8) Zhao, Z.; Ma, X.; Li, Z.; Lin, Y. S. *J. Membr. Sci.* **2011**, *382*, 82−90.
(9) Hu, Y.; Dong, X.; Nan, J.; Jin, W.; Ren, X.; Xu, N.; Lee, Y. M. *Chem. Commun.* **2011**, *47*, 737−739.
(10) Bétard, A.; Bux, H.; Henke, S.; Zacher, D.; Caro, J.; Fischer, R. A. *Microporous Mesoporous Mater.* **2012**, *150*, 76−82.
(11) Ben, T.; Lu, C.; Pei, C.; Xu, S.; Qiu, S. *Chem. - Eur. J.* **2012**, *18*, 10250−10253.
(12) Guo, H.; Zhu, G.; Hewitt, I. J.; Qiu, S. *J. Am. Chem. Soc.* **2009**, *131*, 1646−1647.
(13) Zhao, Z.; Ma, X.; Kasik, A.; Li, Z.; Lin, Y. S. *Ind. Eng. Chem. Res.* **2013**, *52*, 1102−1108.
(14) Wang, W. J.; Dong, X. L.; Nan, J. P.; Jin, W. Q.; Hu, Z. Q.; Chen, Y. F.; Jiang, J. W. *Chem. Commun.* **2012**, *48*, 7022−7024.
(15) Zhang, Y.; Feng, X.; Li, H.; Chen, Y.; Zhao, J.; Wang, S.; Wang, L.; Wang, B. *Angew. Chem., Int. Ed.* **2015**, *54*, 4259−4263.
(16) Morris, W.; Doonan, C. J.; Furukawa, H.; Banerjee, R.; Yaghi, O. M. *J. Am. Chem. Soc.* **2008**, *130*, 12626−12627.
(17) Li, Y. S.; Liang, F. Y.; Bux, H.; Feldhoff, A.; Yang, W. S.; Caro, J. *Angew. Chem., Int. Ed.* **2010**, *49*, 548−551.
(18) Li, Y.; Liang, F.; Bux, H.; Yang, W.; Caro, J. *J. Membr. Sci.* **2010**, *354*, 48−54.
(19) Bux, H.; Liang, F. Y.; Li, Y. S.; Cravillon, J.; Wiebcke, M.; Caro, J. *J. Am. Chem. Soc.* **2009**, *131*, 16000−16001.
(20) Bux, H.; Feldhoff, A.; Cravillon, J.; Wiebcke, M.; Li, Y. S.; Caro, J. *Chem. Mater.* **2011**, *23*, 2262−2269.
(21) Brown, A. J.; Brunelli, N. A.; Eum, K.; Rashidi, F.; Johnson, J. R.; Koros, W. J.; Jones, C. W.; Nair, S. *Science* **2014**, *345*, 72−75.
(22) Huang, A. S.; Bux, H.; Steinbach, F.; Caro, J. *Angew. Chem., Int. Ed.* **2010**, *49*, 4958−4961.
(23) Huang, A. S.; Dou, W.; Caro, J. *J. Am. Chem. Soc.* **2010**, *132*, 15562−15564.
(24) Huang, A. S.; Caro, J. *Angew. Chem., Int. Ed.* **2011**, *50*, 4979−4982.
(25) Huang, A. S.; Wang, N.; Kong, C.; Caro, J. *Angew. Chem., Int. Ed.* **2012**, *51*, 10551−10555.
(26) Huang, A. S.; Chen, Y.; Wang, N.; Hu, Z.; Jiang, J.; Caro, J. *Chem. Commun.* **2012**, *48*, 10981−10983.
(27) Wang, N.; Liu, Y.; Qiao, Z.; Diestel, L.; Zhou, J.; Huang, A. S.; Caro, J. *J. Mater. Chem. A* **2015**, *3*, 4722−4728.
(28) Uribe-Romo, F. J.; Hunt, J. R.; Furukawa, H.; Klöck, C.; O'Keeffe, M.; Yaghi, O. M. *J. Am. Chem. Soc.* **2009**, *131*, 4570−4571.
(29) Côté, A. P.; Benin, A.; Ockwig, N.; Matzger, A.; O'Keeffe, M.; Yaghi, O. M. *Science* **2005**, *310*, 1166−1170.
(30) Hao, D.; Zhang, J.; Lu, H.; Leng, W.; Ge, R.; Dai, X.; Gao, Y. *Chem. Commun.* **2014**, *50*, 1462−1464.
(31) Spitler, E. L.; Koo, B. T.; Novotney, J. L.; Colson, J. W.; Uribe-Romo, F. J.; Gutierrez, G. D.; Clancy, P.; Dichtel, W. R. A. *J. Am. Chem. Soc.* **2011**, *133*, 19416−19421.
(32) Colson, J. W.; Woll, A. R.; Mukherjee, A.; Levendorf, M. P.; Spitler, E. L.; Shields, V. B.; Spencer, M. G.; Park, J.; Dichtel, W. R. *Science* **2011**, *332*, 228−231.
(33) Colson, J. W.; Mann, J. A.; DeBlase, C. R.; Dichtel, W. R. *J. Polym. Sci., Part A: Polym. Chem.* **2015**, *53*, 378−384.
(34) DeBlase, C. R.; Hernández-Burgos, K.; Silberstein, K. E.; Rodriguez-Calero, G. G.; Bisbey, R. P.; Abruna, H. D.; Dichtel, W. R. *ACS Nano* **2015**, *9*, 3178−3183.
(35) Li, Z.; Feng, X.; Zou, Y.; Zhang, Y.; Xia, H.; Liu, X.; Mu, Y. *Chem. Commun.* **2014**, *50*, 13825−13828.
(36) Li, X.; Zang, H.; Wang, J.; Wang, J.; Zhang, H. *J. Mater. Chem. A* **2014**, *2*, 18554−18561.
(37) Shinde, D. B.; Kandambeth, S.; Pachfule, P.; Kumar, R. R.; Banerjee, R. *Chem. Commun.* **2015**, *51*, 310−313.
(38) Zhang, W.; Jiang, P.; Wang, Y.; Zhang, J.; Zhang, P. *Catal. Sci. Technol.* **2015**, *5*, 101−104.
(39) DeBlase, C. R.; Silberstein, K. E.; Truong, T.-T.; Abruna, H. D.; Dichtel, W. R. *J. Am. Chem. Soc.* **2013**, *135*, 16821−16824.
(40) Wall, T. F. *Proc. Combust. Inst.* **2007**, *31*, 31−47.
(41) Ku, A. Y.; Kulkarni, P.; Shisler, R.; Wei, W. *J. Membr. Sci.* **2011**, *367*, 233−239.
(42) Franz, J.; Scherer, V. *J. Membr. Sci.* **2010**, *359*, 173−183.
(43) Robeson, L. M. *J. Membr. Sci.* **1991**, *62*, 165−185.
(44) Robeson, L. M. *J. Membr. Sci.* **2008**, *320*, 390−400.
(45) Ranjan, R.; Tsapatsis, M. *Chem. Mater.* **2009**, *21*, 4920−4924.
(46) De Santis, G.; Fabbrizzi, L.; Licchelli, M.; Poggi, A.; Taglietti. *Angew. Chem., Int. Ed. Engl.* **1996**, *35*, 202−204.
(47) Wind, J. D.; Paul, D. R.; Koros, W. J. *J. Membr. Sci.* **2004**, *228*, 227−236.
(48) Lu, C.; Ben, T.; Xu, S.; Qiu, S. *Angew. Chem., Int. Ed.* **2014**, *53*, 6454−6458.

DOI: 10.1021/jacs.6b03348
J. Am. Chem. Soc. 2016, 138, 7673−7680

(49) Nagaraju, D.; Bhagat, D. G.; Banerjee, R.; Kharul, U. K. *J. Mater. Chem. A* **2013**, *1*, 8828−8835.
(50) Cacho-Bailo, F.; Caro, G.; Etxeberría-Benavides, M.; Karvan, O.; Téllez, C.; Coronas, J. *RSC Adv.* **2016**, *6*, 5881−5889.
(51) Brown, A. J.; Johnson, J. R.; Lydon, M. E.; Koros, W. J.; Jones, C. W.; Nair, S. *Angew. Chem., Int. Ed.* **2012**, *51*, 10615−10618.
(52) Yang, T.; Xiao, Y.; Chung, T.-S. *Energy Environ. Sci.* **2011**, *4*, 4171−4180.
(53) Liu, Y.; Hu, E.; Khan, E. A.; Lai, Z. *J. Membr. Sci.* **2010**, *353*, 36−40.
(54) Kanezashi, M.; O'Brien-Abraham, J.; Lin, Y. S. *AIChE J.* **2008**, *54*, 1478−1486.
(55) Aguado, S.; Nicolas, C. H.; Moizan-Baslé, V.; Nieto, C.; Amrouche, H.; Bats, N.; Audebrandd, N.; Farrusseng, D. *New J. Chem.* **2011**, *35*, 41−44.
(56) Shao, L.; Lau, C.-H.; Chung, T.-S. *Int. J. Hydrogen Energy* **2009**, *34*, 8716−8722.
(57) Huang, K.; Dong, Z. Y.; Li, Q. Q.; Jin, W. Q. *Chem. Commun.* **2013**, *49*, 10326−10328.
(58) Li, Y. S.; Bux, H.; Feldhoff, A.; Li, G. L.; Yang, W. S.; Caro. *Adv. Mater.* **2010**, *22*, 3322−3326.
(59) Huang, A.; Liu, Q.; Wang, N.; Zhu, Y.; Caro, J. *J. Am. Chem. Soc.* **2014**, *136*, 14686−14689.
(60) Knebel, A.; Friebe, S.; Bigall, N. C.; Benzaqui, M.; Serre, C.; Caro, J. *ACS Appl. Mater. Interfaces* **2016**, *8*, 7536−7544.
(61) Bennett, T. D.; Cheetham, A. K. *Acc. Chem. Res.* **2014**, *47*, 1555−1562.
(62) Tominaka, S.; Hamoudi, H.; Suga, T.; Bennett, T. D.; Cairns, A. B.; Cheetham, A. K. *Chem. Sci.* **2015**, *6*, 1465−1473.

DOI: 10.1021/jacs.6b03348
J. Am. Chem. Soc. 2016, 138, 7673−7680